

Soft and Smart: Co-nonsolvency-Based Design of Multiresponsive Copolymers

Debashish Mukherji,^{*,†,‡} Mark D. Watson,[¶] Svenja Morsbach,[†] Marc Schmutz,[§] Manfred Wagner,[†] Carlos M. Marques,[§] and Kurt Kremer[†]

[†]Max-Planck Institut für Polymerforschung, Ackermannweg 10, 55128 Mainz, Germany

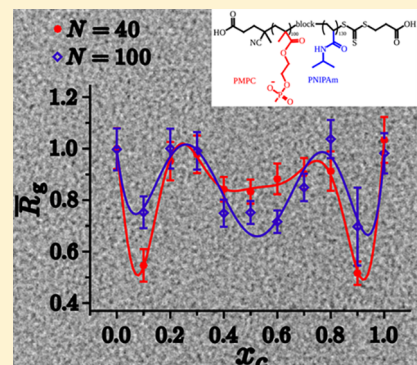
[‡]Stewart Blusson Quantum Matter Institute, University of British Columbia, V6T 1Z4 Vancouver, British Columbia, Canada

[¶]Department of Chemistry, University of Kentucky, 40506-0055 Lexington, Kentucky, United States

[§]Institut Charles Sadron, Université de Strasbourg, CNRS, 67034 Strasbourg, France

Supporting Information

ABSTRACT: A true challenge in designing multiresponsive complex macromolecular architectures is to tune their conformation at will by changing the gradients of external stimuli. However, the lack of a clear molecular-level understanding, establishing a delicate interplay between segment-based interaction details and large-scale macromolecular properties, has hindered the implementation of design principles for a long time. Combining molecular simulations, together with complementary polymer synthesis and characterization, we propose a molecular-level design principle of multiresponsive copolymer architectures. For this purpose, we use the co-nonsolvency concept that is associated with polymer collapse in miscible good solvents. We show how the responsiveness of different polymer blocks can provide fully flexible conformational tuning and, therefore, may serve as a guiding principle for smart material design.



1. INTRODUCTION

Systems that are responsive to external stimuli, such as cosolvent concentration, temperature, pH, and light, are at the onset of many developments in modern classes of soft, smart functional materials.^{1–5} In this context, polymers, whose properties are intimately linked to large conformational and compositional fluctuations, are of paramount importance. Furthermore, when the property of a polymer drastically changes by a slight change of external stimuli, they are referred to as smart responsive polymers. One of the most intriguing phenomenon of smart polymers is co-nonsolvency.^{6–23} Co-nonsolvency occurs when a polymer collapses within intermediate mixing ratios of two miscible and individually good solvents for the very same polymer. While the phenomenon of co-nonsolvency of smart polymers is known for almost three decades now,^{7,8} the origin of this collapse transition is a matter of intense debate. In this context, there are different mechanisms proposed to be driving the transition based on solvent–cosolvent interactions,^{7,20,21} cooperativity effects,^{11,12} preferential binding,^{2,6,9,14,15,22} and kosmotropic effects.¹⁷

There is a broad range of polymers that show co-nonsolvency. Examples include poly(*N*-isopropylacrylamide) (PNIPAm),^{7,8,10,13,14,16} poly(acryloyl-L-proline methyl ester) (PAPOMe),²⁴ and poly(2-(methacryloyloxy)-ethylphosphorylcholine) (PMPC),^{25,26} to list a few.

Smart responsive polymers have a wide range of applications in designing advanced functional materials,^{27–30} such as

biomedical encapsulation,^{31,32} artificial muscle tissues,^{29,33,34} “pick-up and place” systems,³⁵ and biomedical glues.³⁰ However, this requires a rather predictive and highly tunable responsiveness of these “smart” systems, which is not at all trivial in homopolymer systems. Therefore, a possible alternative is to use a copolymer where the properties of different blocks can be tuned at will by changing the external stimuli. In this context, a wide range of copolymers were designed that includes sequences of thermoresponsive smart polymers,^{36–39} copolymer sequences of smart and standard polymers,^{40,41} conventional copolymers,⁴² pluronic,^{31,32} and/or elastin-based peptides.^{1,43}

To the best of our knowledge, studies usually deal with temperature effects.^{31,32,36,37,44–46} This temperature responsiveness is not only restricted to polymers displaying lower critical solution (LCST) temperatures,^{36,37,46} but also with diblock copolymers having one block with LCST behavior and another block displaying upper critical solution (UCST) behavior.⁴⁴ These studies display switchable micellization with changing temperatures. Another interesting route to induce conformational transition of PNIPAm-based copolymers is to have distinct tacticity of different blocks.⁴⁵ Here, it should be noted that tacticity often changes the LCST behavior of a polymer because of the modification of the

Received: February 28, 2019

Revised: April 9, 2019

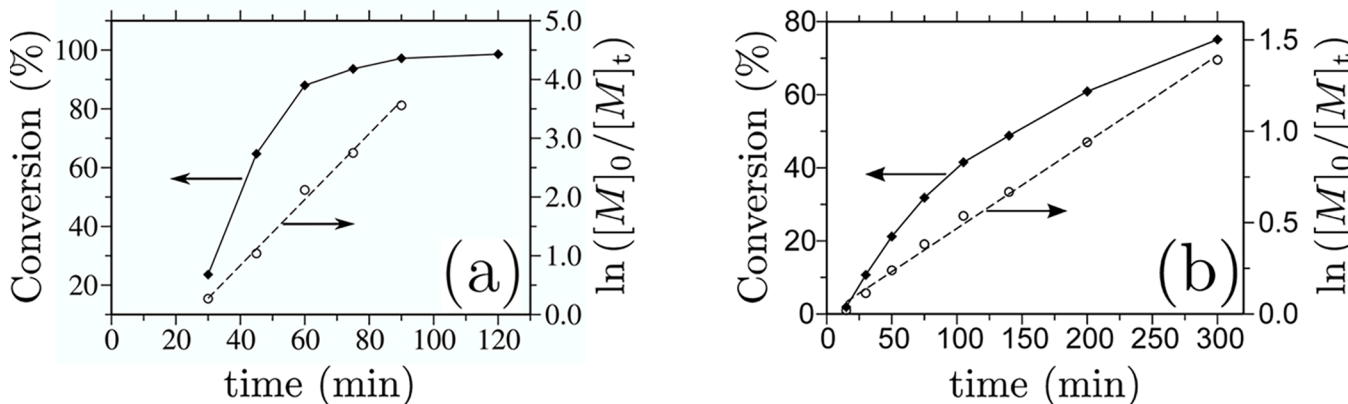


Figure 1. Conversion (monitored via ^1H NMR) as a function of time and pseudo first-order plot for RAFT polymerization of the PMPC block (a) and subsequent PNIPAm block (b).

solvation structure around the amide group of PNIPAm.⁴⁷ Here, however, these copolymer sequences often require large temperature differences, especially for any application in the biomedical context. Therefore, in this unified study, using molecular dynamics simulations and complementary polymer synthesis and characterization, in combination with the concept of co-nonsolvency, we propose an approach applicable to a wide range of copolymer architectures in mixtures of (co)solvents at a given temperature.

2. METHOD, MODEL, AND MATERIALS

Our systems consist of a diblock copolymer and block copolymers showing tunable conformational behavior in solvent mixtures. For this study, we employ a generic polymer model.⁴⁸ For this purpose, we use the idea of preferential binding of one of the (co)solvents with the polymer as the driving force of polymer collapse under the co-nonsolvency condition, as proposed earlier.^{2,16} While the generic principle presented here is not restricted to specific soft materials, for the proof of concept, we also perform experiments on a block copolymer of PNIPAm and PMPC (poly(NIPAm-co-MPC)) in aqueous alcohol mixtures. To identify the conformation of poly(NIPAm-co-MPC) aqueous alcohol mixtures, we have performed polymer synthesis, dynamic light scattering, and cryo-TEM measurements.

Beyond, the generic simulations, details of specific choices of the parameters in simulations, and experimental details are described herein.

2.1. Molecular Dynamics Simulations and Model Parameters. All simulations are based on the well-known bead-spring polymer model.⁴⁸ In this model, individual monomers of a polymer interact with each other via a repulsive 6-12 Lennard-Jones (LJ) WCA potential, with the interaction energy of $\epsilon_p = 1.0\epsilon$ and particle size of $\sigma_p = 1.0\sigma$. All units are expressed in terms of the LJ energy ϵ , LJ radius σ , and mass m of individual monomers. This leads to a time unit of $\tau = \sigma\sqrt{m/\epsilon}$. Additionally, adjacent monomers of a polymer are connected by a finitely extensible nonlinear elastic potential (FENE), $V_{\text{FENE}}(r) = 0.5kR_0^2 \ln\left[1 - \left(\frac{r}{R_0}\right)^2\right]$ for $r \leq R_0$, where $R_0 = 1.5\sigma$ and $k = 30\epsilon/\sigma^2$. The parameters of the potential are such that a reasonably large time-step can be chosen, while bond crossing remains forbidden.

A bead-spring polymer (p) is solvated in mixed solutions composed of two components, the solvent (s) and cosolvent (c), also modeled as LJ beads. Following the protocol in our earlier works,² we chose the sizes of the (co)solvent molecules as $\sigma_{s/c} = 0.5\sigma$, which is half the monomer size σ . As it appears, the solvent sizes dictate the energy density within the solvation volume, and this asymmetry in sizes is important to mimic monomer–solvent interactions, where monomers are usually larger than the solvent components. A copolymer consists

of two kinds of monomers, types a and b , with different monomer sequences. Interactions between different monomer types and (co)solvent components can either be attractive (full LJ 6-12 potential) or repulsive (truncated and shifted LJ interaction).² In the case of attractive interactions, the interaction energy ϵ_{ij} for various pairs is varied and $\sigma_{ij} = 0.75\sigma$, while for the repulsive interactions, $\epsilon_{ij} = 1.0\epsilon$ is kept constant and $\sigma_{ij} = 0.5\sigma$. The details of these specific interaction cases will be discussed in the manuscript whenever appropriate. (Co)solvent particles always repel each other with a repulsive LJ, with $\epsilon_{ij} = 1.0\epsilon$ and $\sigma_{ij} = 0.5\sigma$, which ensures that the solvent–cosolvent mixtures are well miscible with an effective interaction parameter of $\chi = 0$.

The cosolvent mole fraction x_c is varied from 0 (pure s component) to 1 (pure c component). We consider polymer chains with three different degrees of polymerization $N = 30, 40$, and 100 solvated in $2.0 \times 10^4, 2.5 \times 10^4$, and 10×10^4 solvent molecules, respectively. The equations of motion are integrated using a velocity Verlet algorithm with a time-step of $\delta t = 0.01\tau$ and damping coefficient of $\Gamma = 1.0\tau^{-1}$ for the Langevin thermostat. Temperature is set to $T = 0.5\epsilon/\kappa_B$, where κ_B is the Boltzmann constant. The initial configurations are equilibrated for typically several $5 \times 10^4\tau$, which is at least an order of magnitude larger than the longest relaxation time in the system. After this initial equilibration, averages are taken over another $5 \times 10^5\tau$ to obtain observables.

2.2. Dynamic Light Scattering. For light scattering experiments, a commercially available instrument from ALV GmbH was used consisting of an electronically controlled goniometer and ALV-5004 multiple tau full-digital correlator (320 channels). As a light source, a HeNe laser with a wavelength of 632.8 nm and output power of 25 mW (JDS Uniphase, type 1145P) was applied. All sample solutions were filtered through Millex-LCR 0.45 mm filters (Merck Millipore) directly into dust-free quartz light scattering cuvettes (inner diameter: 18 mm), which were cleaned before with distilled acetone in a Thurmond apparatus. For the dynamic light scattering (DLS) experiments, block copolymer samples were dissolved at a concentration of 1 g L^{-1} in pure water and in pure ethanol. All other samples were then prepared by mixing appropriate ratios of stock solutions. The light scattering measurements were then performed at a constant temperature of 20 °C. The Z-average diffusion coefficients were determined after angular dependent measurements and extrapolated to $q \rightarrow 0$.

2.3. Gel Permeation Chromatography. Gel permeation chromatography (GPC) data were collected from a PSS SECurity Agilent 1260 Infinity setup (Polymer Standards Service GmbH (PSS), Mainz, Germany) with a flow rate of 1 mL min^{-1} (aqueous 0.1 M NaNO_3 , 25 °C) through a Suprema Linear M column from PSS and Shodex RI 101 detector. The system was calibrated with linear PEO standards.

2.4. Nuclear Magnetic Resonance. The experiments were accomplished with a 5 mm TXI $^1\text{H}/^{13}\text{C}/^{15}\text{N}/\text{D}$ z-gradient on the 850

MHz spectrometer with a Bruker Avance III system. For ^1H NMR measurements, 128 transients were used with a $9\ \mu\text{s}$ long 90° pulse and a 17000 Hz (20 ppm) spectral width together with a recycling delay of 15 s. The temperature was kept at 293 K and defined with a standard ^1H methanol NMR sample. The control of the temperature was realized with a VTU (variable temperature unit) and an accuracy of ± 0.1 K, which was checked with the standard Bruker Topspin 3.1 software.

2.5. Polymer Synthesis. Monomer 2-methacryloyloxyethyl phosphorylcholine (MPC, Aldrich, 97%) was recrystallized by slow cooling ($70\ ^\circ\text{C} \rightarrow -20\ ^\circ\text{C}$) of a solution in anhydrous acetonitrile containing the minimal amount of anhydrous methanol (1% v/v) to achieve a clear solution at $70\ ^\circ\text{C}$. Monomer *N*-isopropylacrylamide (NIPAM, Aldrich, 97%) was recrystallized by pouring a gently warmed benzene solution into pentane (benzene:pentane $\approx 1:10$) and slowly cooling to $0\ ^\circ\text{C}$. The RAFT agent, 4-(((2-carboxyethyl)-thio)carbonothioyl)thio)-4-cyanopentanoic acid, (Boron Molecular, U.S.A., product number BM1433) and initiator 1,2-bis(2-(4,5-dihydro-1*H*-imidazol-2-yl)-propan-2-yl)diazene dihydrochloride (VA044, Aldrich) were stored in a $-30\ ^\circ\text{C}$ freezer and used as received. Polymerizations were conducted in D_2O . A schematic of the chemical reaction is shown in Figure S2.

2.5.1. Growth of the PMPC Block. MPC (1.95 g, 6.6 mmol, 100 equiv) was weighed inside a nitrogen-filled glovebox and placed in a tared 20 mL Schlenk tube, which was sealed with a rubber septum and removed to a Schlenk line. RAFT agent BM1433 (20.3 mg, 0.066 mmol, 1 equiv) and initiator VA-044 (16 mg, 0.049 mmol, ~ 0.7 equiv) were weighed in open air and added to the Schlenk flask. The vessel was immersed in an ice bath, 10 mL degassed D_2O was added via syringe and the reaction mixture was sparged with nitrogen for 30 min. Polymerization was carried out in a $44\ ^\circ\text{C}$ oil bath under nitrogen. Aliquots were periodically removed via syringe for NMR and GPC analyses, immediately diluted with D_2O , and stored in a refrigerator until analysis. After 2 h, the reaction vessel was cooled in an ice bath. ^1H NMR indicated essentially quantitative conversion (see plot of conversion as a function of time in Figure 1 and the corresponding tabulated data in Tables S-I and S-II). Approximately 11.5 g of the original solution remained, corresponding to ~ 1.7 g of the polymer based on the original mass of MPC.

2.5.2. Growth of the PNIPAM Block. The Schlenk tube from above was cooled in an ice bath and NIPAM (1.12 g, 9.9 mmol, 150 equiv) was weighed in open air and was added. The reaction mixture was again sparged with nitrogen for 30 min and then placed in a $26\ ^\circ\text{C}$ oil bath with magnetic stirring (after taking a $t = 0$ sample for NMR analysis). Aliquots were taken, and analytical samples were prepared as described above until 5 h of reaction time ($\sim 75\%$ conversion). D_2O was removed relatively rapidly under reduced pressure. The gummy residue was dissolved in 10 mL MeOH and dripped into rapidly stirring ether to precipitate. The supernatant was decanted, and the remaining solid was washed with ether. The precipitation/washing was repeated once, and the remaining solid was placed under reduced pressure overnight, see NMR spectra in Figure 3 and tabulated data in Tables S-I and S-II.

2.6. Cryo-TEM Measurements. A laboratory-built humidity-controlled vitrification system was used to prepare the samples for cryo-TEM. Humidity was kept close to 80% for all experiments and the temperature was set at $22\ ^\circ\text{C}$. Five microliters of the sample was placed onto a grid covered by lacey carbon film (Ted Pella), which was rendered hydrophilic via a glow discharge (Elmo, Cordouan Technologies). Excess sample was removed by blotting with filter paper, and the sample grid was vitrified by rapid plunging into liquid ethane ($-160\ ^\circ\text{C}$). The grids were kept in liquid nitrogen before being transferred into a Gatan 626 cryo-holder. Cryo-TEM imaging was performed on a FEI Tecnai G2 TEM (200 kV) under low-dose conditions with an Eagle slow scan CCD camera.

3. RESULTS AND DISCUSSION

3.1. Conformation of the Diblock Copolymer.

We start our discussion by proposing the design principle of the diblock

copolymer sequences consisting of monomer types a and b that respond differently to the same external stimulus. For this purpose, we consider a polymer chain of length N consisting of $N_a = N/2$ monomers of type a having preferential binding with the cosolvent “c”, and the other half, $N_b = N - N_a$ monomers of type b have preferential binding with the solvent “s”. Therefore, polymers with monomers of type a show co-nonsolvency at lower mole fractions of cosolvent (x_c), while polymers with monomers of type b show co-nonsolvency for higher x_c values.² Note, for the simplicity of parameterization, the generic interaction parameters of a with both s and c are taken as they are for PNIPAm in aqueous alcohol mixtures,² while interaction parameters for b with s is varied and will be described whenever needed. Figure 2 presents simulation data

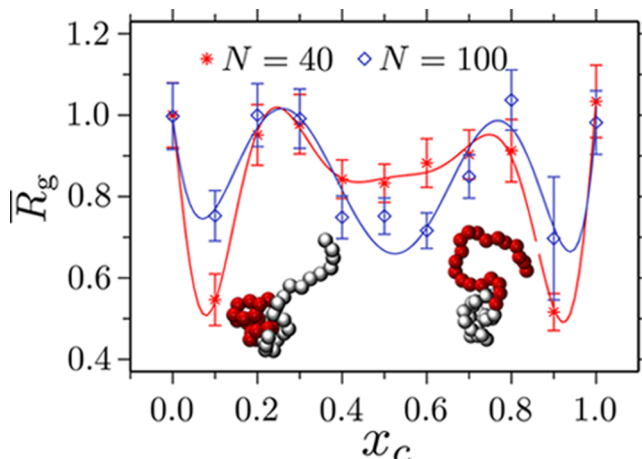


Figure 2. Normalized radius of gyration $\bar{R}_g = R_g/R_g^\circ$ for a diblock copolymer as a function of cosolvent molar fraction x_c . Data is shown for two different chain lengths of N , as shown in the figure legend. Solvent (s) particles have preferential binding with monomer type b, and cosolvent c has preferred interaction with monomer type a. For simplicity of modeling, all interactions are taken as repulsive except of monomer type b with s and monomer type a with c. Attractive interaction strengths are chosen as $\epsilon_{as} = \epsilon_{bc} = 1.0\epsilon$. The lines are polynomial fits to the data that are drawn to guide the eye. Two simulation snapshots are shown for $N = 40$ and for $x_c = 0.1$ when monomer type b collapses (red beads) and for $x_c = 0.9$ when monomer type a collapses (silver beads).

of diblock copolymer conformation in mixed solvents. The data is shown for normalized radius of gyration $\bar{R}_g = R_g/R_g^\circ$ as a function of x_c for two different N values. It can be seen that diblock copolymers can show either double well-like conformational transitions or even multiple minima-type conformational transitions depending on their chain length. The observation of two minima at lower and higher concentrations of cosolvent is not surprising given that two different copolymer segments collapse maximally through two domains of x_c (see simulation snapshots in the inset of Figure 2). A more elaborate phase diagram is shown in Figure S1.

One of the most important aspects of these architectures is that they present fully flexible generic tuning of the conformational behavior, which can be modulated almost at will. In this context, the variation of parameters in molecular simulations is rather simple, especially when dealing with generic models.⁴⁸ Therefore, to study the predicted conformational behavior of diblock copolymers as a function of x_c

having competing structures, we have also synthesized a diblock copolymer.

The choice of a specific chemical system requires a couple of important considerations: (1) Two blocks showing co-nonsolvency in the different regions of the solvent–cosolvent mole fractions: one in the solvent-rich region and another in the cosolvent-rich region, as shown in Figure 2. (2) The most important requirement is that these individual blocks should be responsive to the same solvent–cosolvent mixtures. In this context, one pair of the ideal candidates, though not restricted, for such polymeric blocks are PNIPAm and PMPC chemical structures. For example, under ambient conditions, PNIPAm precipitates between 5–50% ethanol mole fractions,^{7,8} while PMPC exhibits a collapse between 40–90%.^{25,26} If a copolymer is synthesized with these specific blocks, one expects to observe double-well conformational behavior like that predicted in the simulations, see Figure 2. For this purpose, we have synthesized a P(NIPAm-co-MPC) with 130 repeat units of NIPAm and 100 units of MPC using the reversible addition–fragmentation chain-transfer polymerization (RAFT) as shown in Figure 3.

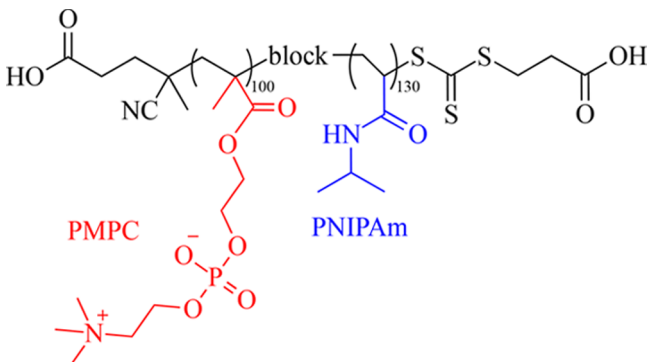


Figure 3. Schematic representation of the chemical structure of a P(NIPAm-co-MPC) diblock copolymer consisting of 100 monomers of MPC and 130 monomers of NIPAm.

To identify conformational behavior in solution, we have first performed dynamic light scattering, where we estimated the hydrodynamic radius R_h of the diblock systems. For pure water $x_c = 0.0$, we find $R_h = 5.6$ nm and for pure ethanol $x_c = 1.0$, $R_h = 5.5$ nm. For the chain lengths chosen here, this corresponds to an expanded configuration of a single chain structure. For $x_c = 0.74$, we observe large structures with $R_h = 22.5$ nm, thus indicating the formation of aggregates. It should also be mentioned that the MD simulations are performed for a single chain, while experimental data is collected with finite polymer concentrations. Therefore, when the polymer conformation shows collapsed structure in simulations, at finite concentrations, this can lead to aggregates.³⁶ Furthermore, as identified by the simulations and based on the well-known behavior of PMPC aqueous alcohol mixtures,^{25,26} inner cores of micelles are formed by the MPC blocks for higher alcohol concentrations, while NIPAm units are forming the outside shell. On the other hand, for $x_c < 0.5$, the inner core is PNIPAm-rich with outer PMPC blocks. We have also tried DLS for $x_c = 0.10$, which however became nontrivial for a low polymer concentration because of the zwitterionic nature of the PMPC block.

To further investigate the possible structure of the copolymer, we have performed cryo-TEM experiments at x_c

= 0.04 and $x_c = 0.74$, see also Section 2.6 for details on cryo-TEM. Images for the two cosolvent mole fractions displayed in Figure 4 clearly show both cases of polymer aggregates compatible with micellar dimensions, highlighted with white arrows. The most prominent view of the micellar objects are observed in the regions of maximum contrast. Especially, the regions with black dots, highlighted by the arrows in Figure 4, indicate micellar objects and reveals the collapsed part of micelles, as reported earlier for micelles made from amphiphilic diblock copolymers.⁴⁹ Note that the soluble parts of the diblock copolymers are not easy to visualize using cryo-TEM. Figure S4 shows two full-field images of cryo-TEM at ethanol volume fractions $x_c = 0.04$ and $x_c = 0.74$. It should also be noted that here, we discuss the generic behavior of a rather large class of systems, even when the experimental proof of concept is restricted to a P(NIPAm-co-MPC) system. Therefore, a rather broad and wide range of chemical systems are expected to show this behavior.

According to simulations, the conformational transitions of the diblock copolymer have strong chain length effects. It can be seen that the multiminima-like behavior is only observed for $N = 100$ (typical of the order of 100 in persistence length l_p), which deserves more attention (see data in blue in Figure 2). This multiminima behavior can be understood by analyzing the co-nonsolvency of corresponding homopolymer blocks of a diblock copolymer in a binary solution.² When a polymer collapses in a mixture of two good solvents, the solvent quality remains good or even gets increasingly better by the addition of a better cosolvent.¹⁶ A data that somewhat speaks in this favor is the ever decreasing variation in excess chemical potential μ_p as a function of x_c (for example, see Figure 5 in ref 16). This suggests that the conformational transition of a polymer in good solvent mixtures is not a phase transition in a true thermodynamic sense.¹⁹ It was previously proposed that while the initial collapse of a homopolymer at around $x_c \rightarrow 0$ is first order-like, the reopening shows inverse system size effects at higher x_c values. The longer the chain, the smoother the reopening transition.² However, it should be noted that the observation of conformational transition discussed here is based on the flexible chain regime. For oligomers (or for very stiff polymers), it will become energetically costlier to form segmental loops, and thus a single rigid chain may not show polymer collapse. Moreover, this may lead to other interesting behaviors at a finite polymer concentration, that is, liquid crystalline or even crystalline ordering mediated by cosolvents. In Figure 5, we show the \bar{R}_g of individual blocks of a diblock with lengths $N_a = N_b = 50$. A smooth reopening is evident from the data. It can be seen that in the $0.35 < x_c < 0.65$ range, both blocks of a diblock copolymer are collapsed, hence the polymer as a whole shows a dip in \bar{R}_g at around $x_c \approx 0.5$ (see Figure 2). Moreover, within the ranges $0.2 < x_c < 0.4$ and $0.6 < x_c < 0.8$, only one of the blocks is collapsed, while the other block remains completely expanded. In combination, this results in the two peaks in \bar{R}_g at around $x_c = 0.3$ (solvent-rich) and 0.7 (cosolvent-rich) in Figure 2.

3.2. Conformation of the Copolymer Sequence. To further study the sequence-dependent design of copolymer architectures, we have also studied the conformation of copolymers with different sequences, that is, with sequence lengths n_s of the two monomer types a and b repeated along the chain length $N = N_a + N_b$. In Figure 6, we show the conformational behavior of the copolymer of $N = 100$ for different n_s values. It can be appreciated that depending on the

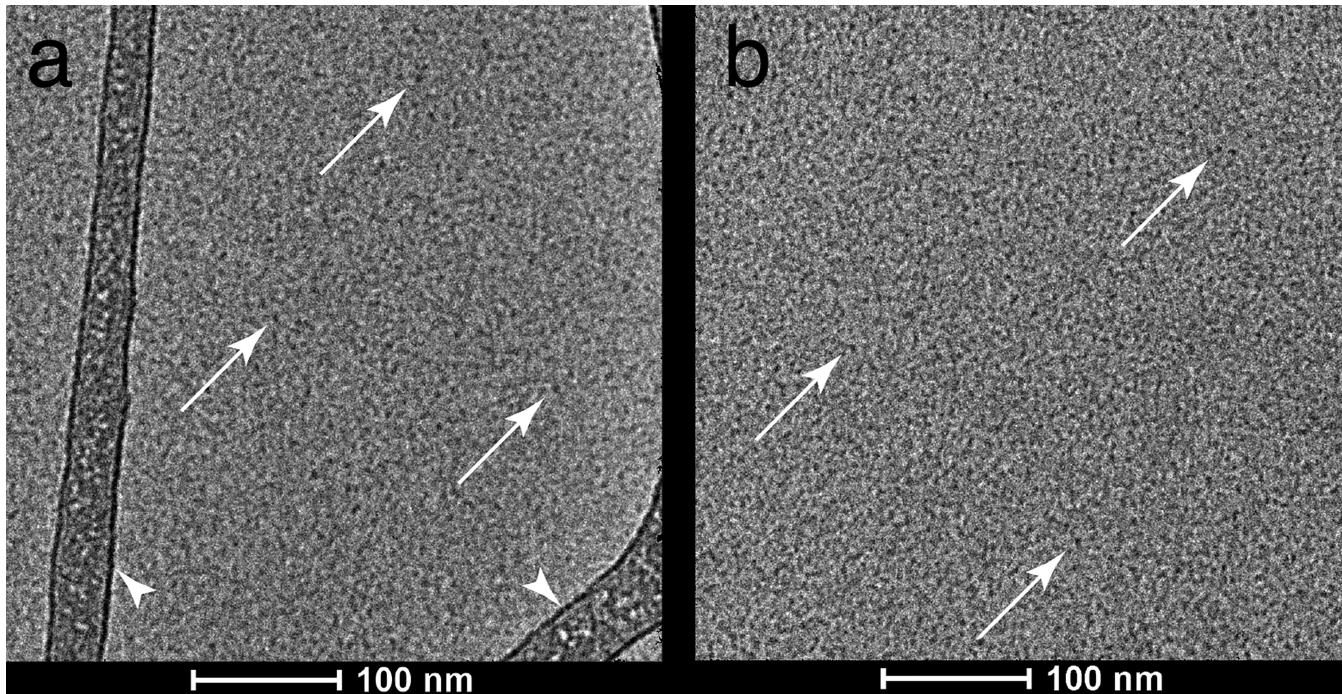


Figure 4. Cryo images of P(NIPAm-co-MPC) for two ethanol volume fractions, (a) $x_c = 0.04$ and (b) $x_c = 0.74$. The core of the polymer micelles are seen as black dots pointed by the arrows. The sample is homogeneously distributed in the amorphous ice layer spanning a supporting carbon/formvar film. The latter is seen in (a) highlighted by the arrowheads.

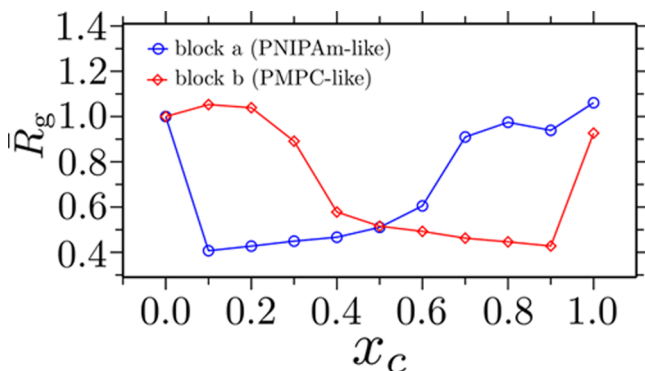


Figure 5. Normalized radius of gyration $\bar{R}_g = R_g/R_g^\circ$ as a function of the cosolvent molar fraction x_c for individual blocks of a diblock copolymer with length $N = 100$. For simplicity of modeling, all interactions are taken as repulsive except those of monomer type b with s and monomer type a with c. Attractive interaction strengths are chosen as $\varepsilon_{as} = \varepsilon_{bc} = 1.0\varepsilon$.

lengths of the sequences, we can find qualitatively different response schemes.

In this last section, we now examine if having only one of the two monomers to be responsive to an external stimulus can still show a re-entrant collapse-swelling transition. In Figure 7, we present data when only monomer type b is responsive, that is, showing co-nonsolvency at lower x_c values. It can be seen from the simulation data that even when only 50% of the monomers have preferential coordination with the cosolvent, copolymers still exhibit co-nonsolvency. For comparison, we also include simulation data of a generic PNIPAM homopolymer in a mixed solvent² that shows good agreement with the present data. Furthermore, a relevant experimental system representing this situation is a random copolymer consisting of NIPAm and DEAm monomers.³⁹ Note that even when a

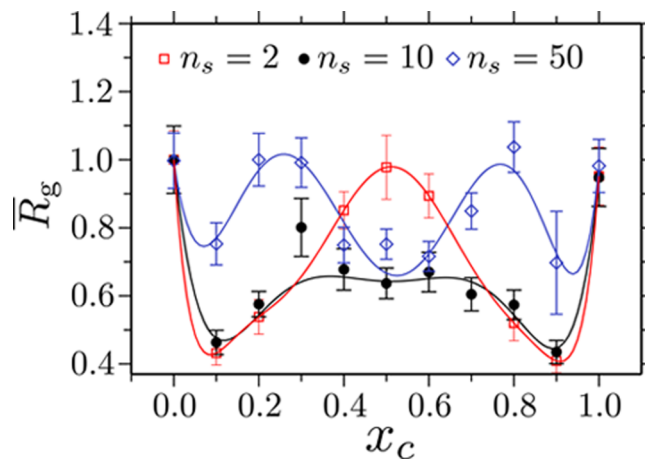


Figure 6. Normalized radius of gyration $\bar{R}_g = R_g/R_g^\circ$ as a function of the cosolvent molar fraction x_c and for the copolymer of length $N = 100$. Results are shown for three different sequences of n_s values. Here, $n_s = 50$ represents the diblock copolymer. The lines are polynomial fits to the data that are drawn to guide the eye.

PDEAm shows a similar temperature effect as PNIPAM, PDEAm does not show co-nonsolvency in an aqueous methanol mixture.³⁹ In Figure 7, we also include the experimental data of a copolymer made from NIPAm and DEAm monomers represented by P(NIPAm-co-DEAm).³⁹ A good agreement between simulation results with the experimental data in Figure 7 presents a situation that the simulation data captured the correct conformational behavior of the reference experimental system. It still is important to mention that the experimental system consists of a statistical random copolymer, while we have a well-defined sequence. Moreover, as it appears, the coil–globule–coil scenario is qualitatively rather independent of the polymer sequence, and

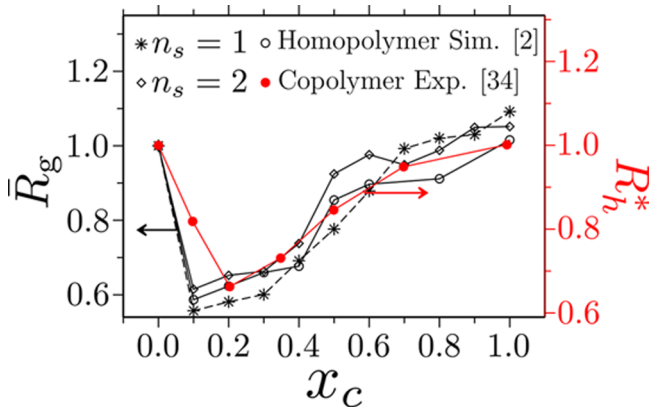


Figure 7. Normalized radius of gyration $\bar{R}_g = R_g/R_g^\circ$ as a function of the cosolvent molar fraction x_c for a copolymer of length $N = 30$. Results are shown for two different copolymer sequences of n_s values, that is, $n_s = 1$ corresponds to an $-(a-b)-$ sequence, and $n_s = 2$ gives an $-(aa-bb)-$ sequence. For comparison, we have also included the generic simulation data corresponding to a homopolymer of PNIPAm² and also the experimental data of P(NIPAm-co-DEAm) taken from ref 39.

a few well-dispersed monomers with preferential binding to one of the cosolvents are sufficient to exhibit the co-nonsolvency effect.

4. CONCLUSIONS

We have proposed a flexible design principle of a set of smart multiresponsive copolymer architectures in mixtures of two good solvents. For this purpose, we have combined generic molecular dynamics simulations and polymer synthesis and characterization to establish a structure–property relation of polymers in mixed solvent mixtures. Results show that the polymer conformation can be tuned at will so long as we choose correct combinations of solvents and copolymer sequences. While it is rather easy to vary parameter space in simulations that can therefore be used to predict a broad range of interesting polymer structures, the predictions are supported with empirical data from a diblock copolymer of PNIPAm and PMPC. This study shows that the different (competing) monomer responsiveness with solvent–cosolvent can be combined to predict structures for desired applications. For example, the architectures presented here are not only interesting, they also possess great technological implications especially in biomedical applications in encapsulation through micellization of polymers. Furthermore, these structures can be extended to account for a combination of thermal and solvent concentration effects within one unified framework, which will be presented elsewhere. Additionally, the conformational transition can also be introduced by changing pH⁵⁰ and thus provide another route to tune conformational behavior. Therefore, in a broad sense, this study may pave new directions toward the operational design and functional application of multiresponsive smart polymeric materials.

■ ASSOCIATED CONTENT

S Supporting Information

The Supporting Information is available free of charge on the ACS Publications website at DOI: [10.1021/acs.macromol.9b00414](https://doi.org/10.1021/acs.macromol.9b00414).

Phase diagram of the copolymer conformations in mixtures of solvents, details on polymer synthesis, cryo measurements ([PDF](#))

■ AUTHOR INFORMATION

Corresponding Author

*E-mail: debashish.mukherji@ubc.ca; mukherji@mpip-mainz.mpg.de.

ORCID

Svenja Morsbach: [0000-0001-9662-8190](https://orcid.org/0000-0001-9662-8190)

Carlos M. Marques: [0000-0002-3952-0498](https://orcid.org/0000-0002-3952-0498)

Kurt Kremer: [0000-0003-1842-9369](https://orcid.org/0000-0003-1842-9369)

Author Contributions

D.M., C.M.M., and K.K. designed the research; D.M. parameterized the generic models, performed numerical simulations, analyzed the data, and proposed the p(MPC-co-NIPAm) system; M.D.W. synthesized p(MPC-co-NIPAm) and wrote the synthesis part in the Method section; S.M. analyzed the light scattering and GPC data and wrote the DLS part in the Method section; M.S. and C.M.M. performed cryo-TEM experiments and wrote the TEM part in the Method section; M.W. performed the NMR measurements and wrote the NMR part in the Method section; and D.M. and K.K. wrote the manuscript.

Notes

The authors declare no competing financial interest.

■ ACKNOWLEDGMENTS

We thank Christine Rosenauer for the DLS and GPC measurements. D.M. thanks Torsten Stuehn for stimulating discussions related to the ESPResSo++ molecular dynamics package,⁵¹ which was used for the simulations in this manuscript. We further acknowledge the microscopy facility at the ICS-CNRS for making their instruments available for the cryo measurements. We thank Robinson Cortes-Huerto, Manjesh Kumar Singh, and Jörg Rottler for critical reading of the manuscript. Snapshots in this manuscript are rendered using VMD.⁵²

■ REFERENCES

- (1) Stuart, M. A. C.; Huck, W. T. S.; Genzer, J.; Müller, M.; Ober, C.; Stamm, M.; Sukhorukov, G. B.; Szleifer, I.; Tsukruk, V. V.; Urban, M.; Winnik, F.; Zauscher, S.; Luzinov, I.; Minko, S. Emerging applications of stimuli-responsive polymer materials. *Nat. Mater.* **2010**, *9*, 101.
- (2) Mukherji, D.; Marques, C. M.; Kremer, K. Polymer collapse in miscible good solvents is a generic phenomenon driven by preferential adsorption. *Nat. Commun.* **2014**, *5*, 4882.
- (3) Halperin, A.; Kröger, M.; Winnik, F. M. Poly(N-isopropylacrylamide) Phase Diagrams: Fifty Years of Research. *Angew. Chem., Int. Ed.* **2015**, *54*, 15342.
- (4) Zhang, Q.; Hoogenboom, R. Polymers with upper critical solution temperature behavior in alcohol/water solvent mixtures. *Prog. Polym. Sci.* **2015**, *48*, 122.
- (5) Mukherji, D.; Marques, C. M.; Stuehn, T.; Kremer, K. Depleted depletion drives polymer swelling in poor solvent mixtures. *Nat. Commun.* **2017**, *8*, 1374.
- (6) Magda, J. J.; Fredrickson, G. H.; Larson, R. G.; Helfand, E. Dimensions of a polymer chain in a mixed solvent. *Macromolecules* **1988**, *21*, 726.
- (7) Schild, H. G.; Muthukumar, M.; Tirrell, D. A. Cononsolvency in mixed aqueous solutions of poly(N-isopropylacrylamide). *Macromolecules* **1991**, *24*, 948.

- (8) Winnik, F. M.; Ringsdorf, H.; Venzmer, J. Methanol-water as a co-nonsolvent system for poly(N-isopropylacrylamide). *Macromolecules* **1990**, *23*, 2415.
- (9) Winnik, F. M.; Ottaviani, M. F.; Bossmann, S. H.; Garcia-Garibay, M.; Turro, N. J. Consolvency of poly(N-isopropylacrylamide) in mixed water-methanol solutions: a look at spin-labeled polymers. *Macromolecules* **1992**, *25*, 6007.
- (10) Zhang, G.; Wu, C. Reentrant Coil-to-Globule-to-Coil Transition of a Single Linear Homopolymer Chain in a Water/Methanol Mixture. *Phys. Rev. Lett.* **2001**, *86*, 822.
- (11) Tanaka, F.; Koga, T.; Winnik, F. M. Temperature-Responsive Polymers in Mixed Solvents: Competitive Hydrogen Bonds Cause Cononsolvency. *Phys. Rev. Lett.* **2008**, *101*, No. 028302.
- (12) Tanaka, F.; Koga, T.; Kojima, H.; Xue, N.; Winnik, F. M. Preferential Adsorption and Co-nonsolvency of Thermoresponsive Polymers in Mixed Solvents of Water/Methanol. *Macromolecules* **2011**, *44*, 2978.
- (13) Kojima, H.; Tanaka, F.; Scherzinger, C.; Richtering, W. Temperature dependent phase behavior of PNIPAM microgels in mixed water/methanol solvents. *J. Polym. Sci., Part B: Polym. Phys.* **2013**, *51*, 1100.
- (14) Walter, J.; Sehrt, J.; Vrabec, J.; Hasse, H. Molecular Dynamics and Experimental Study of Conformation Change of Poly(N-isopropylacrylamide) Hydrogels in Mixtures of Water and Methanol. *J. Phys. Chem. B* **2012**, *116*, 5251.
- (15) Heyda, J.; Muzdalo, A.; Dzubiella, J. Rationalizing Polymer Swelling and Collapse under Attractive Cosolvent Conditions. *Macromolecules* **2013**, *46*, 1231–1238.
- (16) Mukherji, D.; Kremer, K. Coil-globule-coil transition of PNIPAM in aqueous methanol: Coupling all-atom simulations to semi-grand canonical coarse-grained reservoir. *Macromolecules* **2013**, *46*, 9158.
- (17) Bischofberger, I.; Calzolari, D. C. E.; Trappe, V. Co-nonsolvency of PNIPAM at the transition between solvation mechanisms. *Soft Matter* **2014**, *10*, 8288.
- (18) Kyriakos, K.; Philipp, M.; Lin, C.-H.; Dyakonova, M.; Vishnevetskaya, N.; Grillo, I.; Zaccione, A.; Miasnikova, A.; Laschewsky, A.; Müller-Buschbaum, P.; Papadakis, C. M. Quantifying the Interactions in the Aggregation of Thermoresponsive Polymers: The Effect of Cononsolvency. *Macromol. Rapid Commun.* **2016**, *37*, 420.
- (19) Mukherji, D.; Marques, C. M.; Stuehn, T.; Kremer, K. Co-nonsolvency: Mean-field polymer theory does not describe polymer collapse transition in a mixture of two competing good solvents. *J. Chem. Phys.* **2015**, *142*, 114903.
- (20) Dudowicz, J.; Freed, K. F.; Douglas, J. F. Communication: Consolvency and cononsolvency explained in terms of a Flory-Huggins type theory. *J. Chem. Phys.* **2015**, *143*, 131101.
- (21) Jia, D.; Zuo, T.; Rogers, S.; Cheng, H.; Hammouda, B.; Han, C. C. Re-entrance of Poly(N,N-diethylacrylamide) in D₂O/d-Ethanol Mixture at 27°C. *Macromolecules* **2016**, *49*, 5152.
- (22) Backes, S.; Krause, P.; Tabaka, W.; Witt, M. U.; Mukherji, D.; Kremer, K.; von Klitzing, R. Poly(N-isopropylacrylamide) microgels under alcoholic intoxication: When a LCST polymer shows swelling with increasing temperature. *ACS Macro Lett.* **2017**, *6*, 1042.
- (23) Dalgicdir, C.; Rodríguez-Ropero, F.; van der Vegt, N. F. A. Computational Calorimetry of PNIPAM Cononsolvency in Water/Methanol Mixtures. *J. Phys. Chem. B* **2017**, *121*, 7741.
- (24) Hiroki, A.; Maekawa, Y.; Yoshida, M.; Kubota, K.; Katai, R. Volume phase transitions of poly(acryloyl-L-proline methyl ester) gels in response to water-alcohol composition. *Polymer* **2001**, *42*, 1863.
- (25) Kiritoshi, Y.; Ishihara, K. Preparation of cross-linked biocompatible poly(2-methacryloyloxyethyl phosphorylcholine) gel and its strange swelling behavior in water/ethanol mixture. *J. Biomater. Sci., Polym. Ed.* **2002**, *13*, 213.
- (26) Kiritoshi, Y.; Ishihara, K. Molecular recognition of alcohol by volume phase transition of cross-linked poly(2-methacryloyloxyethyl phosphorylcholine) gel. *Sci. Technol. Adv. Mater.* **2003**, *4*, 93.
- (27) Chang, D. P.; Dolbow, J. E.; Zauscher, S. Switchable Friction of Stimulus-Responsive Hydrogels. *Langmuir* **2007**, *23*, 250.
- (28) Schmidt, S.; Zeiser, M.; Hellweg, T.; Duschl, C.; Fery, A.; Möhwald, H. Adhesion and Mechanical Properties of PNIPAM Microgel Films and Their Potential Use as Switchable Cell Culture Substrates. *Adv. Funct. Mater.* **2010**, *20*, 3235.
- (29) Lee, H.; Lee, B. P.; Messersmith, P. B. A reversible wet/dry adhesive inspired by mussels and geckos. *Nature* **2007**, *448*, 338.
- (30) Meddahi-Pellé, A.; Legrand, A.; Marcellan, A.; Louedec, L.; Letourneur, D.; Leibler, L. Organ Repair, Hemostasis, and In Vivo Bonding of Medical Devices by Aqueous Solutions of Nanoparticles. *Angew. Chem., Int. Ed.* **2014**, *53*, 6369.
- (31) Adams, M. L.; Lavasanifar, A.; Kwon, G. S. Amphiphilic block copolymers for drug delivery. *J. Pharm. Sci.* **2003**, *92*, 1343.
- (32) Batrakova, E. V.; Kabanov, A. V. Pluronic block copolymers: Evolution of drug delivery concept from inert nanocarriers to biological response modifiers. *J. Controlled Release* **2008**, *130*, 98.
- (33) Cui, S.; Pang, X.; Zhang, S.; Yu, Y.; Ma, H.; Zhang, X. Unexpected Temperature-Dependent Single Chain Mechanics of Poly(N-isopropyl-acrylamide) in Water. *Langmuir* **2012**, *28*, 5151.
- (34) de Beer, S.; Kutnyanszky, E.; Schön, P. M.; Vancso, G. J.; Müser, M. H. Solvent induced immiscibility of polymer brushes eliminates dissipation channels. *Nat. Commun.* **2014**, *5*, 3781.
- (35) Vogel, M. J.; Steen, P. H. Capillarity-based switchable adhesion. *Proc. Natl. Acad. Sci. U. S. A.* **2010**, *107*, 3377.
- (36) Li, C.; Buurma, N. J.; Haq, I.; Turner, C.; Armes, S. P.; Castelletto, V.; Hamley, I. W.; Lewis, A. L. Synthesis and characterization of biocompatible, thermoresponsive ABC and ABA triblock copolymer gelators. *Langmuir* **2005**, *21*, 11026.
- (37) Lutz, J.-F.; Akdemir, Ö.; Hoth, A. Point by point comparison of two thermosensitive polymers exhibiting a similar LCST: is the age of poly (NIPAM) over? *J. Am. Chem. Soc.* **2006**, *128*, 13046.
- (38) Zhou, Y.; Jiang, K.; Song, Q.; Liu, S. Thermo-Induced Formation of Unimolecular and Multimolecular Micelles from Novel Double Hydrophilic Multiblock Copolymers of N,N-Dimethylacrylamide and N-Isopropylacrylamide. *Langmuir* **2007**, *23*, 13076.
- (39) Scherzinger, C.; Lindner, P.; Keerl, M.; Richtering, W. Cononsolvency of Poly(N,N-diethylacrylamide) (PDEAAM) and Poly(N-isopropylacrylamide) (PNIPAM) Based Microgels in Water/Methanol Mixtures: Copolymer vs Core–Shell Microgel. *Macromolecules* **2010**, *43*, 6829.
- (40) Samanta, S.; Bogdanowicz, D. R.; Lu, H. H.; Koberstein, J. T. Polyacetals: Water-Soluble, pH-Degradable Polymers with Extraordinary Temperature Response. *Macromolecules* **2016**, *49*, 1858.
- (41) De Silva, C. C.; Leophairatana, P.; Ohkuma, T.; Koberstein, J. T.; Kremer, K.; Mukherji, D. Sequence transferable coarse-grained model of amphiphilic copolymers. *J. Chem. Phys.* **2017**, *147*, No. 064904.
- (42) Kelley, E. G.; Smart, T. P.; Jackson, A. J.; Sullivan, M. O.; Epps, T. H., III Structural changes in block copolymer micelles induced by cosolvent mixtures. *Soft Matter* **2011**, *7*, 7094.
- (43) Meyer, D. E.; Chilkoti, A. Purification of recombinant proteins by fusion with thermally-responsive polypeptides. *Nat. Biotechnol.* **1999**, *17*, 1112.
- (44) Arotçaréna, M.; Heise, B.; Ishaya, S.; Laschewsky, A. Switching the Inside and the Outside of Aggregates of Water-Soluble Block Copolymers with Double Thermoresponsivity. *J. Am. Chem. Soc.* **2002**, *124*, 3787.
- (45) Hietala, S.; Nuopponen, M.; Kalliomäki, K.; Tenhu, H. Thermoassociating Poly(N-isopropylacrylamide) A-B-A Stereoblock Copolymers. *Macromolecules* **2008**, *41*, 2627.
- (46) Plamper, F. A.; Steinschulte, A. A.; Hofmann, C. H.; Drude, N.; Mergel, O.; Herbert, C.; Erberich, M.; Schulte, B.; Winter, R.; Richtering, W. Toward Copolymers with Ideal Thermosensitivity: Solution Properties of Linear, Well-Defined Polymers of N-Isopropyl Acrylamide and N,N-Diethyl Acrylamide. *Macromolecules* **2012**, *45*, 8021.

- (47) de Oliveira, T. E.; Mukherji, D.; Kremer, K.; Netz, P. A. Effects of stereochemistry and copolymerization on the LCST of PNIPAm. *J. Chem. Phys.* **2017**, *146*, No. 034904.
- (48) Kremer, K.; Grest, G. S. Dynamics of entangled linear polymer melts: A molecular-dynamics simulation. *J. Chem. Phys.* **1990**, *92*, 5057.
- (49) Lin, Z.; Cai, J. J.; Scriven, L. E.; Davis, H. T. Spherical-to-Wormlike Micelle Transition in CTAB Solutions. *J. Phys. Chem.* **1994**, *98*, 5984.
- (50) Zhang, Y.; Furyk, S.; Bergbreiter, D. E.; Cremer, P. S. Specific Ion Effects on the Water Solubility of Macromolecules: PNIPAM and the Hofmeister Series. *J. Am. Chem. Soc.* **2005**, *127*, 14505.
- (51) Halverson, J. D.; Brandes, T.; Lenz, O.; Arnold, A.; Bevc, S.; Starchenko, V.; Kremer, K.; Stuehn, T.; Reith, D. ESPResSo++: a modern multiscale simulation package for soft matter systems. *Comput. Phys. Commun.* **2013**, *184*, 1129.
- (52) Humphrey, W.; Dalke, A.; Schulten, K. VMD: visual molecular dynamics. *J. Mol. Graphics* **1996**, *14*, 33.